Available at www.sciencedirect.com

ScienceDirect

journal homepage: www.elsevier.com/locate/he

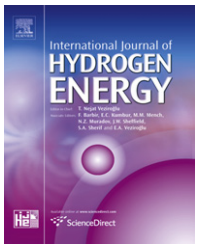

Electronic and bonding properties of MgH_2–Nb containing vacancies

C.R. Luna [a], C.E. Macchi [b,*], A. Juan [c], A. Somoza [d]

[a] IFIMAT, UNCentro and ANPCYT, Pinto 399, B7000GHG Tandil, Argentina
[b] IFIMAT, UNCentro and CONICET, Pinto 399, B7000GHG Tandil, Argentina
[c] Dpto. Física, Universidad Nacional del Sur, Av. Alem 1253, Bahía Blanca, Argentina
[d] IFIMAT, UNCentro and CICPBA, Pinto 399, B7000GHG Tandil, Argentina

ARTICLE INFO

Article history:
Received 25 June 2010
Received in revised form
25 August 2010
Accepted 26 August 2010
Available online 21 September 2010

Keywords:
Magnesium hydride
First principle calculations
Electronic structure
Vacancies

ABSTRACT

The magnesium hydride stability and bonding have been studied using density functional theory (DFT). To this aim, calculations on the electronic structure were performed. We also modeled the bulk hydride with a Nb atom as a substitutional impurity. Furthermore, both systems were modeled containing different types of vacancies (Mg, H or H–Mg complex). The crystal orbital overlap population for both the metal–metal and metal–hydrogen bonds was also computed. The influence of vacancy-like defects was studied through the calculation of the positron lifetimes in defected MgH_2 and defected MgH_2–Nb. For the pure hydride, the results show an increment in the atom bonds in correlation with an increase of the positron localization reflected in a rise of the positron lifetimes. On the other hand, in all considered cases for Mg or/and H vacancies, the presence of Nb reduces the hydride bond about 36%. This decrease in the hydride stability was associated with a decrease in the probability of the positron localization and a consequently reduction of the positron lifetimes.

1. Introduction

It is well known that the use of fossil fuels produces environmental compromise, the CO_2 emission contributes to global warming and the availability of oil reserves around the globe is related to geopolitical tensions. These issues stimulate the study of renewable and clean energy sources to replace the use of fossil fuels [1–3]. Hydrogen is a suitable energy vector to be used for the new economy. However, there are several technological problems that need to be solved, among them hydrogen storage on solid-state materials that chemically bind or physically absorb hydrogen at densities greater than the liquid phase [4]. Among light metals, magnesium hydride is considered one of the most promising candidates for the reversible hydrogen storage due to its low price and high weight percent storage (7.6 wt.%). However, its slow hydrogenation and de-hydrogenation kinetics and the requirement of high temperatures (~300 °C) for its decomposition are the major shortcomings for mobile applications. To solve this problem, it has been proposed to dope MgH_2 with transition metals (TM), such as Nb, Sc, Ti, V, Y and Zr. Specifically, the transition metals act as catalysts reducing the desorption temperature [5–8]. In fact, understanding the microscopic mechanisms linked to the hydrogenation and de-hydrogenation processes are of utmost importance for industrial applications.

There is an interesting number of experimental and theoretical studies considering MgH_2 and MgH_2–Nb [5–16]. Song

* *Corresponding author*. Tel.: +54 2293 439670; fax: +54 2293 439679.
E-mail address: cmacchi@exa.unicen.edu.ar (C.E. Macchi).
0360-3199/$ – see front matter © 2010 Professor T. Nejat Veziroglu. Published by Elsevier Ltd. All rights reserved.
doi:10.1016/j.ijhydene.2010.08.111

et al. [10] studied the influence of the doping elements on the MgH_2 stability. These authors found a decrease in the heat of the MgH_2-X formation being X = Cu, Ni, Al, Nb, and Fe to Ti. This destabilization was attributed to a weakening of the Mg–H bonding. On the other hand, Xiao et al. [14] reported a decrease in the formation enthalpy of MgH_2-TM. They also analyzed the structural and electronic effects on these hydrides.

As known the diffusion in solids is mediated by vacancy-like defects. Specifically, the microscopic mechanisms operating in the hydrogenation and de-hydrogenation of magnesium hydride are related to the formation and diffusivity of vacancies in bulk MgH_2 [17]. Therefore, it is essential to understand the role of the mentioned defects on the electronic and bonding properties. The H vacancy interaction metal has been the objective of several studies [18–21]. Under this frame, the aim of the present work is to study the metal–hydrogen bonding and the effect of the transition metals on the stability of the vacancy–hydride complexes in MgH_2–Nb using first principle calculations. Thus, after generating the crystal structure described in Section 3, *ab initio* calculations were performed to provide information on the energy and electronic structure of the hydrides pure and Nb doped MgH_2, and both structures containing vacancies.

Positron annihilation spectroscopy, mainly positron lifetime technique (PALS) is almost the unique experimental tool to directly obtain information on vacancy-like defects (see a review in Ref. [22]). However, experimental studies on vacancy-like defects in magnesium hydrides are scarce [23–25], any contribution to this issue is of utmost importance. For example, there are no reported theoretical studies. In such a way, the present work is also addressed to the analysis of the structural changes in the hydrides in presence of point defects.

2. Computational method

The energy and electronic structure calculations for the absorption of hydrogen in Mg–Nb were carried out using two computational methods. The first, the atomic superposition and electron delocalization tight-binding (ASED-TB) formalism [26–28], implemented with the YAeHMOP package [29] is described in detail in Refs. [30–32]. Although the method is approximate, it has been used in the present work because it gives a starting point of the main interactions during the absorption process. In fact, the ASED-TB scheme has been successfully used as a comparative tool to study surface and interfacial phenomena in different metals–H systems [33–42].

Table 1 – Atomic parameters for ASED-TB calculation.

Atom	Orbital	IP (Ev)	ξ_1	Ξ_2	c_1	c_2
H	1s	−13.6	1.3			
Mg	3s	−9.0	1.1			
	3p	−4.5	1.1			
Nb	5s	−10.10	1.89			
	5p	−6.86	1.85			
	4d	−12.1	4.08	1.64	0.6401	0.5516

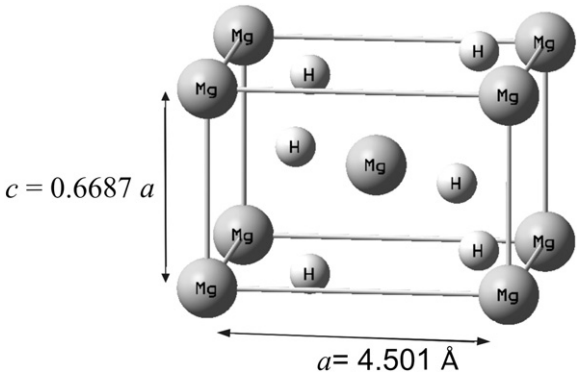

Fig. 1 – Unit cell of MgH_2.

We used as input parameters, a basis set of atomic orbitals and experimental ionization potentials (IP). To obtain a detailed description of the electronic structure properties, we have used a full valence (*s p d*) set of Slater-type orbitals (STO). As usual, in the ASED approximation, single-ζ STO for the *s* and *p* orbitals and double-ζ STO for the *d* orbitals were used. The values of the Slater exponents applied were those optimized for Mg and Nb by Vela and Gázquez [43]. Regarding the experimental valence orbital IP values, which are used as the diagonal elements of the Hamiltonian matrix, spectroscopic data were utilized [44]. In order to minimize exaggerated electron drifts, the IP were adjusted following the same procedure reported in Ref. [45]. The atomic parameters are listed in Table 1.

Additional calculations were carried out within the gradient-corrected density functional theory (GC-DFT) using a supercell containing 48 atomic sites in a tetragonal lattice to model bulk MgH_2 with a $2 \times 2 \times 2$ reciprocal space grid in the supercell Brillouin zone. Specifically, we used the Amsterdam Density Functional 2000 package (ADF-BAND2000) [46]. The molecular orbitals were represented as linear combinations of Slater functions. The gradient correction of the Becke approximation for the exchange energy functional [47] and the B3LYP approximation for the correlation functional were

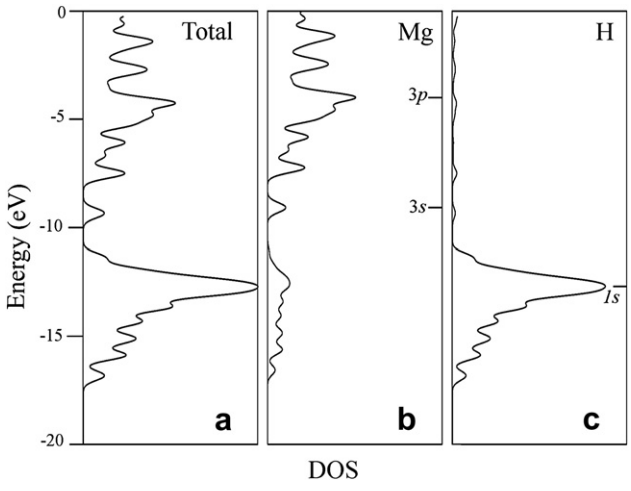

Fig. 2 – (a) Total DOS curves for MgH_2, (b) Projected DOS in a Mg atom, (c) Projected DOS in an H atom. In (b) and (c) the corresponding atomic levels are labeled. $E_F = -11.12$ eV.

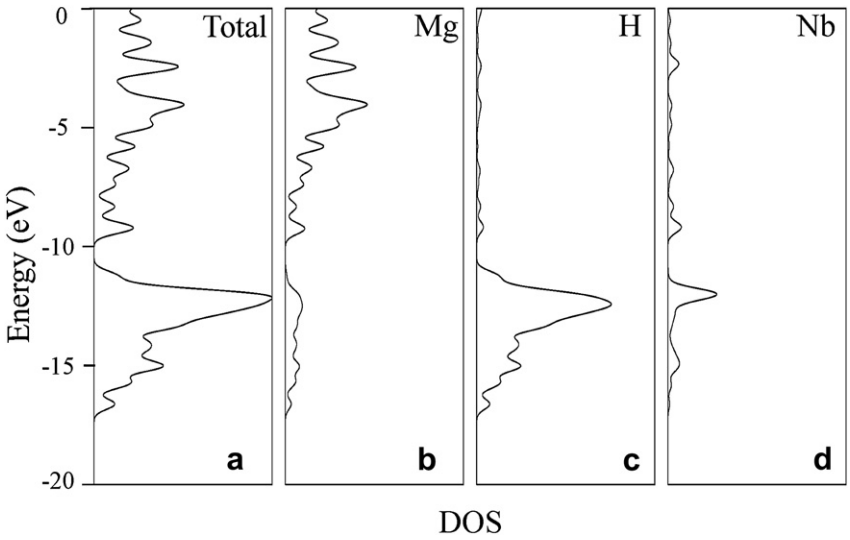

Fig. 3 – (a) Total DOS curves for MgH_2 + Nb, (b) projected DOS in a Mg atom, (c) in an H atom and (d) in a Nb atom. The lines on the right are the corresponding atomic levels. $E_F = -11.90$ eV.

employed [48]. In order to increase the computational efficiency, the innermost atomic shells of electrons were kept frozen for every atom except hydrogen, since the internal electrons do not contribute significantly to the bonding. We have used a triple-zeta basis set with polarization functions to express the atomic orbitals of Mg and Nb. The basis set of Mg consisted of 3*s* and 3*p* orbitals and for Nb 5*s*, 5*p* and 4*d*.

To understand the MgH_2 + Nb interactions we have used the concepts of density of states (DOS) and the overlap population density of states (OPDOS), as described in Refs [33–36].

Table 2 – Overlap population (OP) for the MgH_2 and MgH_2 + Nb systems perfects and with vacancies.

Structure	Bond	Distance (Å)	OP	ΔOP (%)
MgH_2	Mg–Mg	3.520	0.005	–
	Mg–H	1.247	0.595	–
MgH_2–V_H	Mg–Mg		0.005	0
	Mg–H		0.596	0.2
MgH_2–V_{Mg}	Mg–Mg		0	–
	Mg–H		0.622	4.5
MgH_2–V_H–V_{Mg}	Mg–Mg		0	–
	Mg–H		0.632	6.2
MgH_2–Nb	Mg–Mg	3.520	0.012	140
	Mg–H	1.247	0.401	−32.6
	Nb–Mg	3.520	0.045	–
	Nb–H	1.930	0.272	–
MgH_2–Nb–V_H	Mg–Mg		0.019	280
	Mg–H		0.401	−32.6
	Nb–Mg		0.044	−2.2
	Nb–H		0.272	–
MgH_2–Nb–V_{Mg}	Mg–Mg		0.011	120
	Mg–H		0.379	−36.3
	Nb–Mg		0.045	–
	Nb–H		0.258	−5.1
MgH_2–Nb–V_H–V_{Mg}	Mg–Mg		0.018	26
	Mg–H		0.380	−36.1
	Nb–Mg		0.044	−2.2
	Nb–H		0.270	−0.7

To calculate the positron lifetimes we have followed the procedure described in Refs [49–51]. Specifically, we have made our calculations mentioned using the free available Doppler program developed by the Electronic Properties of Materials Research Group at the Helsinki University of Technology [52]. In particular, we have used a two-component Density Functional Theory (DFT) in which the electron density of the solid was approximated by the superposition of free-atom electron densities. The potential felt by the positron was constructed as a sum of the Coulomb and correlation potentials, respectively. Then, positron lifetimes were obtained as the inverse of the annihilation rates calculated as an overlap integral of the electron and positron densities plus a term that takes into account the electron–positron correlation function at the positron site [51]. This term is usually called enhancement factor. Positron lifetimes were calculated using either the local density approximation (LDA) or the Generalized Gradient Approximation (GGA) of the correlation energy. In the first case, the Boronski and Nieminen (BN) approximation for the electron–positron enhancement factor [53] was used. When using GGA, the Arponen–Pajanne approximation [54] for the enhancement factor was utilized. In the case of calculation of the positron lifetimes in the bulk hydrides, only the Γ point of the Brillouin zone was considered. Instead, the lifetimes in vacancies were calculated in the Γ and L points of the Brillouin zone (options allowed into the program Doppler) [52]. In all the positron calculations a mesh of 192 × 192 × 128 grid points was used. For the present work, the tetragonal structure of MgH_2 was modeled using a 384 atoms supercell without atomic position relaxation.

3. Crystal and defect structure

The MgH_2 solid has a tetragonal structure of rutile type (P42/mnm, group No. 136), specified by a lattice parameter *a* and the *c*/*a* ratio (see Fig. 1). The primitive cell has two

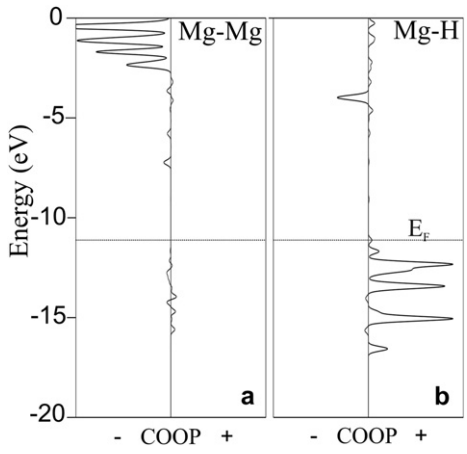

Fig. 4 – COOP curves of MgH_2: (a) Mg–Mg first neighbors and (b) Mg–H.

Mg atoms, one at the origin and the other at the center of the cell at (1/2, 1/2, 1/2) plus four hydrogen atoms at (±x, ±x, 0) and (1/2 ± x, 1/2 ± x, 1/2). The exact values of c/a and x depend on the pressure, at ambient conditions the following reported values $c/a = 0.6687$ and $x = 0.304$ were used [9,55]. Specifically, the presence of an H vacancy (V_H), or a Mg vacancy (V_{Mg}) or an H–Mg mixed vacancy ($V_H - V_{Mg}$) in the pure and niobium-doped magnesium hydride were analyzed. In such a way, V_H and V_{Mg} were introduced removing one H and/or one Mg atom from the center of the cell. Besides, the MgH_2–Nb structure was generated by replacing one Mg atom by another Nb; i.e., the supercell contains 1 Nb atom, 127 Mg atoms and 256 H atoms.

4. Results and discussion

Let us discuss first the electronic structure of pure MgH_2. The total and projected DOS are presented in Fig. 2. The Mg and H based states present similar plots to those reported in Refs. [5,10]. The Mg and H bands present a mixed state between −17 eV to the Fermi level. The Mg *s* and *p* states have a band of 5.94 eV. The Mg *s* states are located between −11.4 eV and −16.9 eV followed by the *p* states up to the Fermi level.

When a Mg atom is replaced by a Nb one, its projected DOS shows a narrow band close to the Fermi level (see Fig. 3). On the other hand, the presence of a vacancy in the studied compounds only changes the Mg p_z orbital occupation. Besides, the Nb substitutional position introduces a de-population in all orbitals nearest neighbors of Mg. The Mg and H states are similar to those presented in Fig. 2.

Table 2 presents the changes in the overlap population (OP) for the different systems studied. The introduction of an H vacancy has almost no effect on the chemical bonds for both Mg–H and Mg–Mg. However, when a Mg vacancy is considered the Mg–H bond increases its OP by 4.5%. If both vacancies are simultaneously considered the main effect still comes from V_{Mg}. When Nb is considered as substitutional to Mg, the Mg–Mg bond increases its OP by 140%, while the Mg–H bond decreases (32.6%) and the Nb–H bond is developed. If H vacancy is added, the Mg–Mg OP becomes greater and no further Mg–H OP decrease is observed. Besides, the Nb–H bond remains unchanged. When a V_{Mg} is considered, the Nb–H OP decreases about 5.1% and when V_{Mg} and V_H are simultaneously introduced the increase of the Mg–Mg OP is only 26%. In all considered cases, containing Nb as substitutional, V_{Mg}, V_H or V_{Mg}–V_H defect strongly reduces the Mg–H bond by 32–36%.

The COOP curves in Figs. 4 and 5b clearly show that the addition of a substitutional Nb reduces the Mg–H OP peaks between −17 eV and E_F while the Nb–H OP is much lower and is not compensated by the loss in the Mg–H bond (see Fig. 5d). This behavior can be interpreted as a destabilization of the MgH_2 cohesion by Nb.

In previous works reported by Barbiellini et al. [54,56], it was concluded that LDA systematically overestimates the annihilation rate while GGA improves the predictive power of positron lifetime calculations over those based on the LDA. For this reason, in the present work positron lifetimes were calculated using GGA. In Table 3, τ values corresponding to positron annihilation in pure Mg and Nb as in the perfect bulk state as well for these pure metals containing single vacancies are presented. Our results show a very good agreement with the lifetimes reported in the literature (see Table 3).

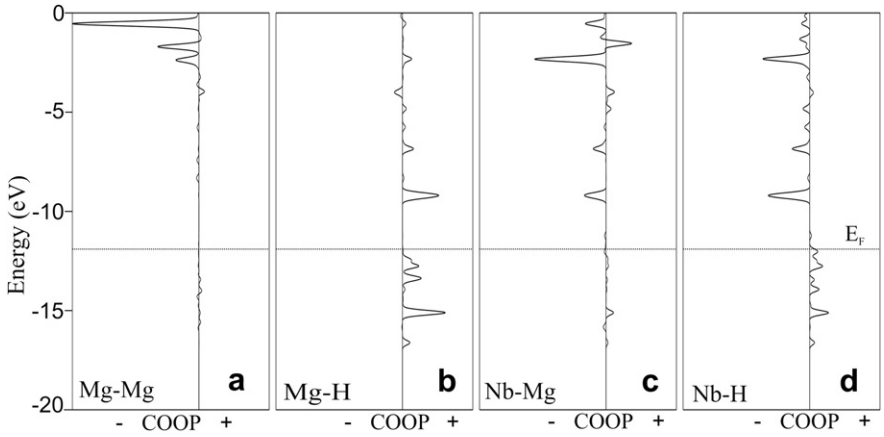

Fig. 5 – COOP curves of the MgH_2 + Nb: (a) Mg–Mg first neighbors, (b) Mg–H, (c) Nb–Mg and (d) Nb–H.

Table 3 – Positron lifetimes in the perfect bulk and in a monovacancy for pure Mg and pure Nb. Lifetime values were calculated using GGA.

Material	Present work		Reported values	
	Bulk	Vacancy	Bulk	VACANCY
Mg	226	292	226[a]	292[a]
Nb	134	224	134[a], 135[b]	224[a], 225[b]

a Ref. [57].
b Ref. [56].

On the other hand, we report in Table 4 the positron lifetimes calculated for magnesium hydride and niobium-doped magnesium hydride. When comparing, negligible differences between the τ values obtained for both bulk materials are observed. Besides, the absolute positron lifetime for MgH_2 is near but slightly lower than that for bulk Mg. The addition of Nb as a dopant to the MgH_2 does not introduce significant changes in the respective τ, despite the lifetime in the perfect Nb is almost 70% lower than that in bulk Mg.

When considering single vacancies in the above mentioned materials, the results obtained depend on the kind of point defect considered for the calculations.

Firstly, we will discuss the results obtained for magnesium hydride. In this case, when this hydride contains a Mg vacancy the positron lifetime increases about 11.5%. When an H vacancy is considered into the MgH_2, a τ increment of approximately 1% is obtained. In the case of a mixed vacancy complex, composed by a Mg vacancy plus an H one, the calculated τ values show a strong increase (~17%).

On the other hand, all the positron lifetime calculated for single vacancies in MgH_2–Nb are systematically below to those obtained for the pure hydride (see in Table 4 the percentage relative lifetime changes with respect to the bulk materials).

Preliminary results of a work in progress we are developing, using a self-consistent calculations, would indicate that the positron lifetime differences between both hydrides containing Mg or H–Mg vacancies can be attributed to the higher electron density around this transition metal.

A final paragraph deserves a joint analysis of the positron results and the electronic and bonding properties of the hydrides studied. When comparing positron lifetimes with the OP results for magnesium hydrides, an increment of the positron lifetime is correlated to an increase in the atom bonds reflected in a better stability of the hydrides. The substitution of a Mg atom by a Nb one in MgH_2 modifies the electronic density around the Nb atom decreasing the positron lifetime and in such a sense the probability of positron localization. As shown in Table 2, this modification can be associated with a decrease in the hydride stability. The same behavior was observed with the hydride systems containing vacancies.

Table 4 – Positron lifetimes calculated for magnesium hydride and niobium-doped magnesium hydride (see details in the text). In the table, the percentage variations (%) in the positron lifetimes taken with respect to that corresponding to the bulk material are also presented.

	Material			
	MgH_2		MgH_2–Nb	
	τ^{GGA}(ps)	%	τ^{GGA}(ps)	%
Bulk	219.5	–	219.2	–
V_{Mg}	244.0	11.5	241.0	10
V_H	221.2	0.9	220.0	0.5
V_H–V_{Mg}	256.6	17	251.4	14.5

5. Conclusions

We have studied the influence of vacancies on the electronic structure, bonding and positron lifetimes in pure magnesium hydride and in niobium-doped magnesium hydride. To this aim, first principle calculations were used to compute the crystal orbital overlap population for both the metal–metal and metal–hydrogen bonds in the perfect MgH_2 and in this material containing a Mg vacancy, an H one or a mixed H–Mg vacancy complex. The same calculations were also performed in the magnesium hydride with a Nb atom as substitutional impurity and on this material containing the same kind of vacancies above mentioned. Simultaneously, the influence of vacancy-like defects in the hydride was studied through the calculation of the positrons lifetime in the previously referred materials.

The main results can be summarized as follows:

i) In all considered cases for Mg or/and H vacancies, the presence of Nb reduces the metal–hydrogen bond about 36%. The combined effect of Mg and H vacancies is close to that for the Mg vacancy. When Nb is considered, a small Nb–H bond is detected but this does not compensate the decrease in the Mg–H bonding.
ii) When comparing the positron lifetimes for MgH_2 and this system with a Nb atom located as a substitutional impurity, no lifetime difference was found.
iii) In the pure magnesium hydride containing an H vacancy, the lifetime only increases approximately 1%. However, this parameter increases about 11% if a Mg vacancy is considered and the strongest increase in the positron lifetime value (~17%) was found for a mixed vacancy complex, composed by a Mg vacancy and an H vacancy.
iv) In MgH_2–Nb containing different kinds of vacancies the calculated positron lifetimes are systematically below to those obtained for the pure hydride
v) The net effect of Nb in bonding is to decrease the MgH_2 stability regardless of the presence of vacancies, as was experimentally found.

Finally, it is important to point out that the results obtained from positron calculations are in agreement with those obtained from DOS and OP curves.

Acknowledgements

This work was partially supported by PICT2006-1650 and PICTR 656/560, Agencia Nacional de Promoción Científica y Tecnológica (Argentina) and PIP 114-200801-00444, Consejo Nacional

de Investigaciones Científicas y Técnicas (Argentina). We acknowledge the useful comments of Drs. P. Jasen and E. González on the analysis of the results obtained on the electronic and bonding properties. A.S. and C.M. acknowledges the valuable help of Dr. I. Makkonen and Dr. P. Folegati in the use of the MIKA code.

REFERENCES

[1] Schlapbach L, Züttel A. Hydrogen-storage materials for mobile applications. Nature 2001;414:353–8.
[2] Cortright RD, Davda RR, Dumesic JA. Hydrogen from catalytic reforming of biomass-derived hydrocarbons in liquid water. Nature 2002;418:964–7.
[3] Rosi NL, Ekert J, Eddaoudi M, Vodak DT, Kim J, O'Keeffe M, et al. Hydrogen storage in microporous metal–organic frameworks. Science 2003;300:1127–9.
[4] Mckamey CG, Devan JH, Tortorelli PF, Sikka VK. A review of recent developments in Fe_3Al-based alloys. J Mater Res 1991; 6:1779–804.
[5] Yu R, Lam PK. Electronic and structural properties of MgH_2. Phys Rev B 1988;37:8730–7.
[6] Shang X, Bououdina M, Guo ZX. Structural stability of mechanically alloyed (Mg + 10Nb) and (MgH_2 + 10Nb) powder mixtures. J Alloys Compd 2003;349:217–23.
[7] Selvam P, Viswanathan B, Swamy CS, Srinivasan V. Magnesium and magnesium alloy hydrides. Int J Hydrogen Energy 1986;11:169–92.
[8] Liang G. Synthesis and hydrogen storage properties of Mg-based alloys. J Alloys Compd 2004;370:123–8.
[9] Pozzo M, Alfé D. Structural properties and enthalpy of formation of magnesium hydride from quantum Monte Carlo calculations. Phys Rev B 2008;77:1–8. 104103.
[10] Song Y, Guo ZX, Yang R. Influence of selected alloying elements on the stability of magnesium dihydride for hydrogen storage applications: a first-principles investigations. Phys Rev B 2004;69:94215–942051.
[11] Song Y, Guo ZX. Metastable MgH_2 phase predicted by first principles calculations. Appl Phys Lett 2006;89: 111911–3.
[12] Shang CX, Bououdina M, Song Y, Guo ZX. Mechanical alloying and electronic simulations of (MgH_2 + M) system (M = Al, Ti, Fe, Ni, Cu and Nb) for hydrogen storage. Int J Hydrogen Energy 2004;29:73–80.
[13] Sato T, Kyoi D, Rönnebro E, Kitamura N, Sakai T, Noréus D. Structural investigations of two new ternary magnesium–niobium hydrides, $Mg_{6.5}NbH_{14}$ and $MgNb_2H_4$. J Alloys Compd 2006;417:230–4.
[14] Xiao XB, Zhang WB, Yu WY, Wang N, Tang BY. Energetic and electronic properties of Mg_7TMH_{16} (TM = Sc, Ti, V, Y, Zr, Nb): an ab initio study. Phys Rev B 2009;404:2234–40.
[15] Gasan H, Aydinbeyli N, Celik ON, Yaman YM. The dependence of the hydrogen desorption temperature of MgH_2 on its structural and morphological characteristics. J Alloys Compd 2009;487:724–9.
[16] Charbonnier J, de Rango P, Fruchart D, Miraglia S, Skryabina N, Huot J, et al. Structural analysis of activated Mg (M)H_2. J Alloys Compd 2005;404–406:541–4.
[17] Park MS, Janotti A, Van de Walle CG. Formation and migration of charged native point defects in MgH_2: first-principles calculations. Phys Rev B 2009;80:1–5. 064102.
[18] Ardenghi S, González E, Jasen P, Juan A. The hydrogen interaction in an FCC FePd alloy with a vacancy. Phys Scripta 2009;79:1–5. 045702.
[19] Ismer L, Park MS, Janetti A, Van de Walle CG. Interactions between hydrogen impurities and vacancies in Mg and Al: a comparative analysis based on density functional theory. Phys Rev B 2009;80:1–10. 184110.
[20] Fukai Y, Sugimoto H. Formation mechanism of defect metal hydrides containing superabundant vacancies. J Phys Condens Matter 2007;19:1–24. 436201.
[21] Hao S, Sholl DS. Selection of dopants to enhance hydrogen diffusion rates in MgH_2 and $NaMgH_3$. Appl Phys Lett 2009;94: 1–3. 171909.
[22] Hautojärvi P, Corbel CJ. In: Dupasquier A, Mills Jr AP, editors. Positron Spectroscopy of Solids. Amsterdam: IOS; 1995. p. 491–532.
[23] Checchetto R, Bazzanella N, Miotello A, Brusa RS, Zecca A, Mengucci A. Deuterium storage in nanocrystalline magnesium thin films. J Appl Phys 2004;95:1989–95.
[24] Eijt SWH, Kind R, Singh S, Schut H, Legerstee WJ, Hendrikx RWA, et al. Positron depth profiling of the structural and electronic structure transformations of hydrogenated Mg-based thin films. J Appl Phys 2009;105:1–13. 043514.
[25] Leegwater H, Schut H, Egger W, Baldi A, Dam B, Eijt SWH. Divacancies and the hydrogenation of Mg-Ti films with short range chemical order. Appl Phys Lett 2010;96:1–3. 121902.
[26] Anderson AB, Hoffmann R. Description of diatomic molecules using one electron configuration energies with two-body interactions. J Chem Phys 1974;60:1–3. 4271.
[27] Anderson AB. Derivation of the extended Hückel method with corrections: one electron molecular orbital theory for energy level and structure determinations. J Chem Phys 1975; 62:1187–8.
[28] Anderson AB. The influence of electrochemical potential on chemistry at electrode surfaces modeled by MO theory. J Electroanal Chem 1990;280:37–48.
[29] Landrum GA, Glassey WV. Yet another extended Hückel molecular orbital package (YAeHMOP). YAeHMOP is freely available on the world wide web at:. CornellUniversity http://yaehmop.sourceforge.net/; 2004.
[30] Hoffmann R, Lipscomb WN. Theory of polyhedral molecules. I. Physical factorizations of the secular equation. J Chem Phys 1962;36:2179–89.
[31] Hoffmann R. An extended Hückel theory. I. Hydrocarbons. J Chem Phys 1963;39:1397–412.
[32] Anderson AB. Electron density distribution functions and the ASED-MO theory. Int J Quantum Chem 1994;49:581–9.
[33] Simonetti S, Rey Saravia D, Brizuela G, Juan A. The effects of a hydrogen pair in the electronic structure of the FCC iron containing a vacancy. Int. J. Hydrogen Energy 2010;35: 5957–66.
[34] Juan A, Moro L, Brizuela G, Pronsato E. The electronic structure and bonding of an hydrogen pair near a FCC Fe stacking fault. Int J Hydrogen Energy 2002;27:333–8.
[35] Gesari SB, Pronsato ME, Juan A. Simulation of hydrogen trapping at defects in Pd. Int J Hydrogen Energy 2009;34:3511–8.
[36] Simonetti S, Moro L, Brizuela G, Juan A. The interaction of carbon and hydrogen in a [alpha]-Fe divacancy. Int J Hydrogen Energy 2006;31:1318–25.
[37] Lopez-Corral I, German E, Volpe MA, Brizuela GP, Juan A. Tight-binding study of hydrogen adsorption on palladium decorated graphene and carbon nanotubes. Int J Hydrogen Energy 2010;35:2377–84.
[38] Jasen P, Gonzalez E, Luna CR, Brizuela G, Juan A. The hydrogen effect in the electronic structure and bonding of the B2 FeAl alloy with a Fe vacancy. Int J Hydrogen Energy 2009;34:9591–5.
[39] Rey Saravia D, Juan A, Brizuela G, Simonetti S. Comparative study of H-atom location, electronic and chemical bonding in ideal and vacancy containing-FCC iron. Int J Hydrogen Energy 2009;34:8302–7.

[40] Simonetti S, Moro L, Gonzalez NE, Brizuela G, Juan A. Quantum chemical study of C and H location in an fcc stacking fault. Int J Hydrogen Energy 2004;29:649–58.
[41] Juan A, Pistonesi C, Garcia AJ, Brizuela G. The electronic structure and bonding of a H–H pair in the vicinity of a BCC Fe bulk vacancy. Int J Hydrogen Energy 2003;28:995–1004.
[42] Jasen P, Gonzalez E, Brizuela G, Nagel OA, Gonzalez GA, Juan A. A theoretical study of the electronic structure and bonding of the monoclinic phase of Mg_2NiH_4. Int J Hydrogen Energy 2007;32:4943–8.
[43] Vela A, Gázquez JL. Extended Hückel parameters from density functional theory. J Phys Chem 1988;92:5688–93.
[44] Lotz W. Electron binding energies in free atoms. J Opt Soc Am 1970;60:206–10.
[45] Anderson AB, McDevitt RM, Urbach FL. Structure and electronic factors in benzene coordination to $Cr(CO)_3$ and to cluster models of Ni, Pt, and Ag (111) surfaces. Surf Sci 1984;146:80–8.
[46] Amsterdam Density Functional Package Release. Amsterdam: Vrije Universiteit; 2001.
[47] Becke D. Density-functional exchange-energy approximation with correct asymptotic behavior. Phys Rev A 1988;38:3098–100.
[48] Lee C, Yang W, Parr RG. Developed of the Colle–Salvetti correlation-energy formula into a functional of the electron density. Phys Rev B 1998;37:785–9.
[49] Puska MJ, Nieminen RM. Theory of positrons in solids and on solid surfaces. Rev Mod Phys 1994;66:841–97.
[50] Torsti T, Heiskanen M, Puska MJ, Nieminen RM. MIKA: a multigrid-based program package for electronic structure calculations. Int J Quantum Chem 2003;91: 171–6.
[51] Torsti T, Eirola T, Enkovaara J, Hakala T, Havu P, Höynälänmaa T, et al. Three real-space discretization techniques in electronic structure calculations. Phys Status Solid B 2006;243:1016–53.
[52] Doppler. A program to model positron states and annihilation in solids. Laboratory of Physics, Helsinki University of Technology, http://tfy.tkk.fi/epm/research/positron/dopplerdoc.pdf; 2003.
[53] Boronski E, Nieminen RM. Electron–positron density–functional theory. Phys Rev B 1986;34:3820–31.
[54] Barbiellini B, Puska MJ, Torsti T, Nieminen RM. Gradient corrections for positron states in solids. Phys Rev B 1995;51: 7341–4.
[55] Bortza M, Berthevillea B, Böttgerb G, Yvona K. Structure of the high pressure phase γ-MgH_2 by neutron powder diffraction. J Alloys Compd 1999;287:L4–6.
[56] Barbiellini B, Puska MJ, Korhonen T, Harju A, Torsti T, Nieminen RM. Calculation of positron states and annihilation in solids: a density-gradient-correction scheme. Phys Rev B 1996;53:16201–13.
[57] Campillo JM, Ogando E, Plazaola F. Positron lifetime calculation for the elements of the periodic table. J Phys Condens Matter 2007;19:1–20. 176222.